Environmental Science Nano

ROYAL SOCIETY OF CHEMISTRY

PAPER

View Article Online
View Journal | View Issue

Check for updates

Cite this: *Environ. Sci.: Nano*, 2021, **8**, 2554

Published on 20 July 2021. Downloaded by Fail Open on 7/23/2025 9:11:29 AM.

Effects of ingested nanocellulose and nanochitosan materials on carbohydrate digestion and absorption in an *in vitro* small intestinal epithelium model†

Zhongyuan Guo,‡[a] Glen M. DeLoid,‡[a] Xiaoqiong Cao,[a] Dimitrios Bitounis,[a] Kaarunya Sampathkumar,[b] Kee Woei Ng,[abcd] Say Chye Joachim Loo[ab] and Philip Demokritou*[ab]

Received 12th March 2021,
Accepted 19th July 2021

DOI: 10.1039/d1en00233c

rsc.li/es-nano

Nanoscale materials derived from natural biopolymers like cellulose and chitosan have many potentially useful agri-food and oral drug delivery applications. Because of their large and potentially bioactive surface areas and other unique physico-chemical properties, it is essential when evaluating their toxicological impact to assess potential effects on the digestion and absorption of co-ingested nutrients. Here, the effects of cellulose nanofibers (CNF), cellulose nanocrystals (CNC), and chitosan nanoparticles (Chnp) on the digestion and absorption of carbohydrates were studied. Starch digestion was assessed by measuring maltose released during simulated digestion of starch solutions. Glucose absorption was assessed by measuring translocation from the resulting digestas across an *in vitro* transwell tri-culture model of the small intestinal epithelium and calculating the area under the curve increase in absorbed glucose, analogous to the glycemic index. At 1% w/w, CNF and Chnp had small but significant effects (11% decrease and 14% increase, respectively) and CNC had no effect on starch hydrolysis during simulated digestion of a 1% w/w rice starch solution. In addition, at 2% w/w CNC had no effect on amylolysis in 1% solutions of either rice, corn, or wheat starch. Similarly, absorption of glucose from digestas of starch solutions (*i.e.*, from maltose), was unaffected by 1% w/w CNF or CNC, but was slightly increased (10%, $p < 0.05$) by 1% Chnp, possibly due to the slightly higher maltose concentration in the Chnp-containing digestas. In contrast, all of the test materials caused sharp increases (~1.2, 1.5, and 1.6 fold for CNC, CNF, and Chnp, respectively) in absorption of glucose from starch-free digestas spiked with free glucose at a concentration corresponding to complete hydrolysis of 1% w/w starch. The potential for ingested cellulose and chitosan nanomaterials to increase glucose absorption could have important health implications. Further studies are needed to elucidate the mechanisms underlying the observed increases and to evaluate the potential glycemic effects in an intact *in vivo* system.

Environmental significance

This article reports findings of studies on the potential effects of ingested nanocellulose and nanochitosan materials on carbohydrate digestion and absorption. While potential applications for these materials in foods and drug delivery grow, our findings suggest their ingestion may have unwanted effects on carbohydrate digestion and particularly on glucose absorption. Such studies provide essential guidance needed by regulators to evaluate the safety of the products that enter our food environment. The food environment plays a major role in the food choices that people make, which in turn have important public health consequences. Here we report *in vitro* findings suggesting that nanocellulose and nanochitosan materials, though not directly toxic and having only small effects on starch digestion and bioavailability, may increase the rate of glucose translocation across the small intestinal epithelium when glucose is ingested directly (*i.e.*, *via* corn syrup in processed foods). In our *in vitro* small intestinal epithelium model we observed increases of 20–60% in the area under the curve (AUC) for translocated glucose (analogous to glycemic index). The introduction of these nanomaterials to foods without further study and consideration of such potential impacts could have a dangerous effect on the food environment, potentially exacerbating an ongoing worldwide obesity crisis and diabetes epidemic.

[a] *Center for Nanotechnology and Nanotoxicology, Department of Environmental Health, Harvard T. H. Chan School of Public Health, Boston, MA 02115, USA. E-mail: pdemokri@hsph.harvard.edu*
[b] *School of Materials Science and Engineering, Nanyang Technological University, 50 Nanyang Avenue, 639798, Singapore, Singapore*
[c] *Skin Research Institute of Singapore, 8A Biomedical Grove, #06-06 Immunos, 138648, Singapore*
[d] *Environmental Chemistry and Materials Centre, Nanyang Environment & Water Research Institute, 1 Cleantech Loop, CleanTech One, Singapore 637141, Singapore*

† Electronic supplementary information (ESI) available. See DOI: 10.1039/d1en00233c

‡ Equally contributing authors: Glen M. DeLoid and Zhongyuan Guo.

This journal is © The Royal Society of Chemistry 2021

Published on 20 July 2021. Downloaded by Fail Open on 7/23/2025 9:11:29 AM.

Introduction

Engineered nanomaterials (ENMs) derived from natural biopolymers, such as cellulose and chitosan, possess unique or enhanced properties (relative to their larger-scale counterparts) that have fueled the development of a large and growing number of new applications for such materials in the agri-food, healthcare, and pharmaceutical industries.[1–10] Cellulose-based ENMs, such as cellulose nanofibrils (CNF) and cellulose nanocrystals (CNC), have potential applications, as biodegradable food packaging materials that could increase shelf life and improve product safety, and more importantly as processed food ingredients, at concentrations ranging from ~0.2% to 1.0% w/w, to provide a non-caloric source of dietary fiber, or to stabilize food emulsions and foams (*e.g.*, sauces, dressings, and toppings), increase moisture retention, or improve sensory qualities.[11–16] In addition, it was recently shown that ingested CNF reduces the digestion and absorption of co-ingested fat, suggesting a potential use for CNF in weight management.[17] Chitosan-based ENMs, particularly nanoscale chitosan particles, have demonstrated great potential as oral drug and nutraceutical delivery platforms, likely due to their polycationic structure at intestinal pH, and resulting mucoadhesive and tight junction disrupting properties, which can facilitate intestinal absorption of orally administered small molecules and peptides.[18–27]

Although bulk or micron-scale natural biopolymer and inorganic materials have long been used and generally regarded as safe in foods at low concentrations, because their counterpart nanoscale materials may exhibit unique properties and biointeractions,[28–35] the safety of these nanoscale materials cannot be assumed to be similar to that of the bulk materials, and must be studied. Several studies have shown that ingestion of inorganic nanoparticles, such as TiO_2, SiO_2, and ZnO, can damage intestinal microvilli and impair nutrient absorption,[36–39] and may cause genotoxicity, tumorigenesis, shifts in gut microbiome, and exacerbation of experimental colitis.[40–45] Likewise, with natural biopolymer nanomaterials, it is essential to understand the potential health impacts of ingestion exposures to the nanoscale forms of these materials, and to provide the relevant toxicological data needed by regulators to evaluate the safety of these materials. Because these materials have unique physico-chemical properties and large surface areas available for potential interactions with nutrients, digestive enzymes and chemicals, or components of the gastrointestinal tract (GIT) mucus or epithelial cell surface, in addition to assessing their direct toxicity, it is important to assess the potential impact that their ingestion might have on digestion and absorption of key nutrients.

We and others have recently published results from studies of the *in vitro* and *in vivo* toxicology of ingested nanocellulose nanomaterials,[46,47] and of the *in vitro* toxicology of ingested chitosan nanoparticles,[48] which revealed few significant adverse effects. In our *in vitro* studies of nanoscale cellulose and chitosan ENMs, a physiological three-phase (oral, gastric, and small intestinal) GIT digestion simulator was employed to digest either water or standardized food model suspensions containing the ENMs at relevant exposure concentrations, and the final small intestinal digestas were applied to a tri-culture small intestinal epithelium cellular model for assessment of toxicity.[46,48–50] The tri-culture model, described and characterized in detail by the authors in an earlier publication, includes Caco-2 cell-derived absorptive enterocytes and microfold (M) cells, and mucus-secreting HT29-MTX cells representing goblet cells and providing a physiological mucus layer.[49] Exposure of the tri-cultures to digestas containing cellulose nanocrystals (CNC) caused a slight (10%) increase in reactive oxygen species (ROS) generation, but did not affect cytotoxicity (LDH release) or monolayer integrity (transepithelial electrical resistance, TEER),[46] and exposure to digestas containing chitosan nanoparticles (Chnp) produced a slight (10%) increase in cytotoxicity (LDH release), but did not diminish TEER or cell viability, or increase oxidative stress (ROS formation).[48] Our *in vivo* studies, in which rats received biweekly gavage treatments with CNF for five weeks, also revealed no adverse effects. Serum chemistry, hematology, and histological analysis of lung, liver, kidney and small intestine identified no significant abnormalities or differences between treatment groups.[46] Our findings are consistent with the results of other studies of such natural biopolymer nanomaterials in the literature, and suggest that their ingestion in small amounts poses little risk of direct toxicity.[51–53]

Although the cellulose and chitosan nanomaterials did not appear in our recent published studies to cause significant direct *in vitro* cytotoxicity, or *in vivo* toxicity in the case of CNF, there are other means by which ingested substances can cause adverse health consequences that would not be detected in typical toxicological studies. These include effects on intestinal epithelial barrier function, the gut microbiome, and nutrient digestion and absorption. For instance, we recently reported that CNF ingestion (gavage) altered fecal microbial diversity, specifically diminishing populations of species that produce short chain fatty acids, and that are linked to increased mucosal IgA production, but had relatively little effect on the microbial metabolism, with significant fold changes seen for only ten metabolites out of 366 measured.[54] Exposure to CNF also altered expression of epithelial cell junction genes and increased production of cytokines that modulate proliferation of CD8 T cells, which may represent initiation of an adaptive immune response.[54]

Ingested nanomaterials also have the potential to alter digestion or absorption of nutrients. We previously reported that ingested nanocellulose materials can significantly reduce the digestion and absorption of fat both *in vitro* and *in vivo*.[17] Scanning electron microscopy and molecular dynamics studies suggested that this effect was due to the coalescence of fat droplets on CNF fibers, resulting in a reduction of available surface area for lipase binding, as well as sequestration of bile salts. Similar findings have also been reported, including significant reduction of TG hydrolysis in sunflower oil-in-water emulsions stabilized with CNC and

Published on 20 July 2021. Downloaded by Fail Open on 7/23/2025 9:11:29 AM.

whey protein, which was attributed to the bridging of multiple fat droplets by CNCs to produce larger droplets with reduced total available surface area.[55] Several studies have found that nanocellulose materials may also influence the digestion of starch, as detailed in a recent review by Liu and Kong.[56] Nsor-Atindana *et al.* found that the presence of CNC significantly decreased digestion and glucose release from a protein–starch system during two stage gastric and small intestinal digestion,[57] and Ji *et al.* reported significant reductions in starch digestibility in the presence of CNC in a simple enzyme–buffer system.[58] The presence of CNF at 0.22 and 1.1% was reported by Liu *et al.* to significantly decrease glucose production from corn starch as well as glucose diffusion in a three phase *in vitro* digestion system.[59] Together these studies suggest that nanocellulose may have a potential hypoglycemic effect when ingested with starch. The results of *in vivo* studies to date are somewhat conflicting. Andrade *et al.* reported no significant effects on blood glucose in rats fed chow containing CNF from peach palm residue at up to 21% by weight for 30 days.[60] In contrast, Chen *et al.* reported that in mice fed on a high fat and sucrose diet (western diet), gavage treatment with wood-derived CNF at 30 mg kg^{-1} body weight for 6 weeks caused a slight but significant reduction in lean body mass as well as non-specifically decreased intestinal absorption (D-xylose absorption) and altered glucose homeostasis.[61]

In the present study, we investigated the effects of both cellulose and chitosan ENMs on the digestion of starch and the absorption of glucose in an *in vitro* cellular model. Simulated three phase (oral, gastric, and small intestinal) digestion and a tri-culture small intestinal epithelial model were employed to assess the effects of CNC and CNF, as well as Chnp, on the gelatinized (cooked) starch digestion (hydrolysis or amylolysis and release of maltose), and on small intestinal epithelial glucose uptake and translocation.

Materials and methods

Nanomaterial fabrication and characterization

Cellulose nanofibrils (CNF) and nanocrystals (CNC). Details of the methods used to synthesize cellulose materials used in this study and their detailed physicochemical and morphological characterization are described by the authors in a separate companion manuscript.[62] Briefly, fibrillar NC materials (CNF-50 nm) were synthesized using mechanical grinding of a wood fiber, and CNC was synthesized by milling with sulfuric acid.

Chitosan nanoparticles. Chitosan nanoparticles (Chnp) were fabricated and physico-chemically characterized as previously described.[63] Chitosan powder (≥75% deacetylated, 50–190 kDa MW) was dissolved at 1% (w/v) chitosan in a 50% (v/v) acetic acid solution, and then electrosprayed directly into a solution of 1% tripolyphosphate (TPP, Sigma-Aldrich) cross-linker and 0.5% (v/v) Tween 80 (Sigma-Aldrich) in water. Particles were collected by centrifugation at 13 000 × *g*, washed three times, freeze-dried, and stored at −20 °C.

Measurement of zeta potential. The zeta potentials (ζ mV) of pristine CNC and CNF suspensions in sterile deionized water at 0.1 mg mL^{-1} were determined by electrophoretic light scattering (ELS) using a Zetasizer Nano-ZS (Malvern Instruments, Ltd.).

Endotoxin and sterility assessment of ENMs. ENMs were tested for endotoxin levels using the EndoZyme® recombinant factor C (rFC) assay (Hyglos, Germany) according to manufacturer's instructions as described in detail by the authors.[62] In Brief, 10 μg mL^{-1} suspensions of ENMs as well as endotoxin standard dilutions and ENM suspensions spiked with 0.5 EU (endotoxin units) per mL were prepared in endotoxin-free water. Samples, spiked samples, and standard dilutions were dispensed into a prewarmed (37 °C) 96 well plate (100 μl per well) and mixed with 100 μl assay reagent (8 : 1 : 1 ratio of assay buffer, enzyme, and substrate). Fluorescence (Ex 380, Em 440) was measured at t = 0 and at 90 minutes. Endotoxin levels were calculated from sample fluorescence using a standard curve equation generated from a range of endotoxin dilutions.

Microbiological sterility of all nanomaterials used was assessed using WHO protocol in the international pharmacopoeia[64] as previously described.[62,65] Briefly, materials were suspended at 1 mg mL^{-1}, and 1 mL of the suspensions were added to 10 mL of fluid thioglycolate medium at pH 6.9–7.3. The solutions were incubated at 37 °C for 14 days and examined each day for indications of bacterial growth. Every third day during incubation samples of broth were spread onto tryptic soy agar plates and mixed with potato dextrose agar and plate count agar to create pour plates. All plates were incubated at 37 °C for 3 days and examined for growth of bacterial and fungal colonies.

***In vitro* gastrointestinal digestion simulation studies.** *In vitro* simulated digestion was performed using a 3-phase (oral, gastric, and small intestinal) simulator as previously described.[49] An overview of the study design is shown in Fig. 1.

Food model preparation for simulated digestion studies. Because Chnp settles rapidly in water, dispersions of Chnp were created by discrete (rather than continuous) sonication, as previously described.[66,67] Briefly, the critical delivered sonication energy (DSE_{cr}), the minimum energy (J mL^{-1}) needed to produce the smallest agglomerates, was determined by incremental sonication and size characterization by dynamic light scattering (DLS) using a Zetasizer Nano ZS (Malvern Instruments LTD, Worcestershire, UK). A 5 mL sample of 30 mg mL^{-1} Chnp in deionized (DI) water was alternately sonicated (using a calibrated sonicator with known energy output in J s^{-1}) for 30 s and vortexed for 10 s, and mean hydrodynamic diameter (d_H) measured by DLS was plotted as a function of time to determine the minimum sonication time, and thus energy (DSE_{cr}), required to achieve the smallest possible d_H. CNF and CNC dispersions were created by diluting as synthesized aqueous stock suspensions (2.5% w/w for CNF and 7.0% w/w for CNC) in DI water and vortexing for 20 s.

 This journal is © The Royal Society of Chemistry 2021

Published on 20 July 2021. Downloaded by Fail Open on 7/23/2025 9:11:29 AM.

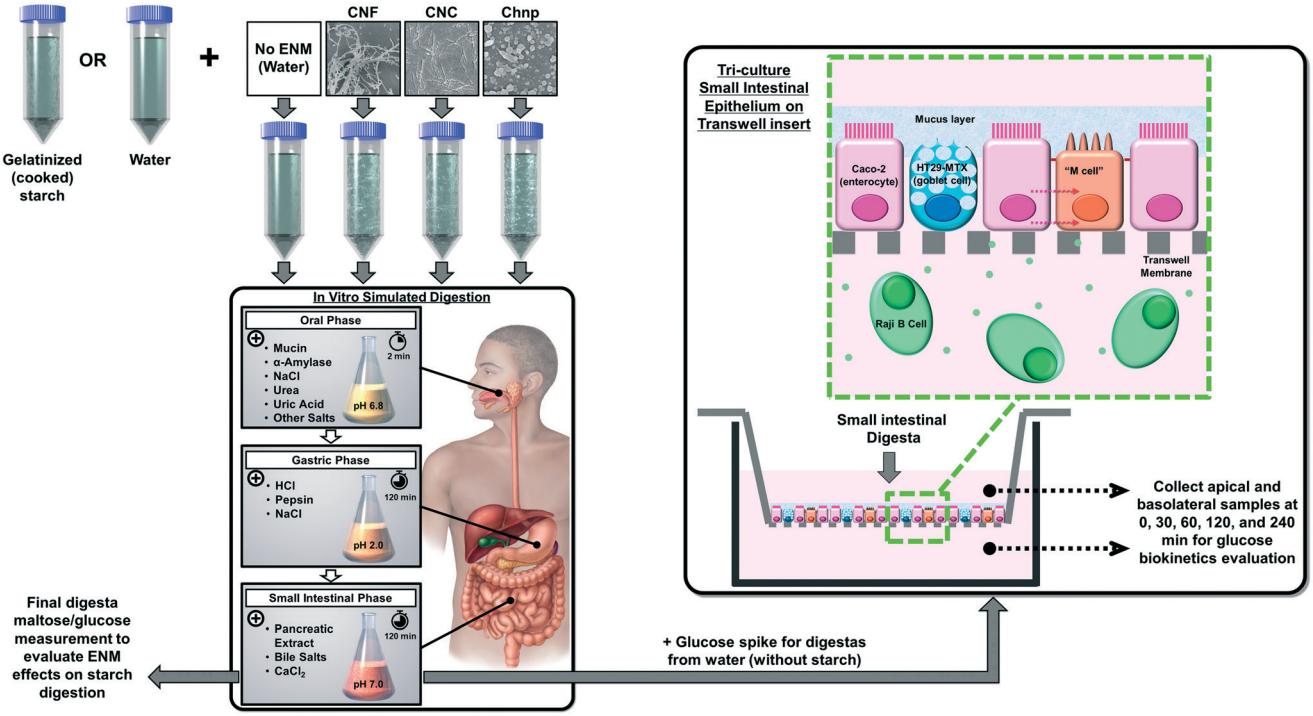

Fig. 1 Study design. ENMs were dispersed in either a gelatinized starch or water only food model (upper left). To assess effects of the ENMs on starch digestion, maltose produced during complete simulated oral, gastric, and small intestinal digestion was measured (lower left). To evaluate effects of ENMs on uptake and translocation of glucose from digested starch (primarily maltose) the digestas from starch were applied to the apical compartments of small intestinal epithelial model transwells, and total glucose in the apical and basolateral compartments were measured over 4 hours. To determine the effects of ENMs on uptake and translocation of free glucose, the final digestas of water without starch were spiked with glucose and applied to the transwell tricultures and apical and basolateral glucose were measured over 4 hours.

Briefly, the materials (CNC, CNF, Chnp) were dispersed at 2% (w/w) in water. 100 mL 2% (w/w) starch solution (rice, corn, wheat) was heated until boiling, then diluted 1 : 1 (to 1% w/w) in 2% (w/w) nanomaterial dispersants, vortexed for 30 seconds to mix, and prewarmed to 37 °C in a water bath. The starch-material mixture was then combined with an equal volume of prewarmed (37 °C) simulated saliva fluid, and mixed by inverting for 10 seconds, representing the oral phase. The resulting oral digesta was then combined 1 : 1 with simulated gastric fluid and incubated for two hours at 37 °C on an orbital shaker at 200 rpm to complete the gastric phase. In the small intestinal phase, the final gastric phase digesta was combined with additional salts, bile extract and pancreatin solution to simulate intestinal fluid, and incubated in an orbital shaker at 200 rpm and 37 °C for 2 hours.

Effects of cellulose and chitosan nanomaterials on starch digestion. To evaluate possible effects of the ENMs on the enzymatic hydrolysis and release of maltose (glucose dimers) in the GIT, we measured free maltose and glucose produced and calculated the percentage of the initial starch digested during simulated digestion of gelatinized starch suspensions with or without ENMs. The final small intestinal digestas were dialyzed to remove solids and proteins: 0.75 mL of digesta was transferred to a 1.5 mL 1 kD dialysis tube, which was submerged in 15 mL of DI water in a 50 mL conical tube and incubated for 48 h at 4 °C. Glucose and maltose in the dialysate were measured using a fluorometric maltose–glucose assay kit (Sigma-Aldrich) according to the manufacturers protocols. The method employs α-D-glucosidase to convert maltose to two glucose monomers, and subsequent oxidation of glucose to produce a fluorescent product (λ_{ex} = 535, λ_{em} = 587). Each dialyzed digesta sample was measured both with and without α-D-glucosidase to differentiate between maltose and free glucose.

Tri-culture small intestinal epithelium cell model and treatments to assess cytotoxicity and absorption of glucose. Small intestinal epithelial model tri-cultures were prepared as previously described.[49] In summary, Caco-2, HT29-MTX, and Raji B cells were obtained from Sigma-Aldrich. Caco-2 and HT29-MTX cells were grown in high-glucose DMEM supplemented with 10% heat-inactivated fetal bovine serum (FBS), 10 mM HEPES buffer, 100 IU mL^{-1} penicillin, 100 μg mL^{-1} streptomycin and non-essential amino acids (1/100 dilution of 100× solution, ThermoFisher). Raji B cells were cultured in RPMI 1640 media supplemented with 10% FBS, 10 mM HEPES buffer, 100 IU mL^{-1} penicillin and 100 μg mL^{-1} streptomycin. For transwell inserts, Caco-2 and HT29-MTX cells were trypsinized and resuspended in DMEM media at 3×10^5 cells per mL and combined in a ratio of 3 : 1 (Caco-2 : HT29-MTX). A 1.5 mL portion of the cell mixture was seeded in the apical chamber, and 2.5 mL of complete DMEM media was added to the basolateral compartment of a 6 well transwell

Published on 20 July 2021. Downloaded by Fail Open on 7/23/2025 9:11:29 AM.

plate (Corning). Media was changed after four days, and subsequently every other day, until day 15. On day 15 and 16, the media in the basolateral compartment was replaced with 2.5 mL of a suspension of Raji B cells at a concentration of 1×10^6 cells per mL in 1 : 1 DMEM : RPMI complete media. Transepithelial electrical resistance (TEER) was measured using an EVOM2 epithelial volt/ohm meter with a Chopstick Electrode Set (World Precision Instruments).

Cytotoxicity (LDH release), and uptake and translocation studies using tri-cultures on transwells were initiated on day 17. Cell viability (tetrazolium salt reduction) and oxidative stress (ROS production) studies require closed-bottom adherent cell cultures in 96-well plates suitable for plate reader fluorescence measurements. For these studies, Caco-2/HT29-MTX co-cultures were prepared in 96-well plates. Raji B cells were not used in this format, since they are suspension feeder cells (added to the transwell basolateral compartments to promote M-cell differentiation of some apical Caco-2 cells), and not part of the epithelium, but could adhere to mucus, or become incorporated in the epithelial layer, if applied apically in closed 96-well plates. To prepare these co-cultures, Caco-2 and HT29-MTX cells at a 3 : 1 ratio were seeded at a total 3×10^4 cells per well (100 μL of cell mixture) in black-walled, clear optical bottom plates (BD Biosciences). Media was changed after four days, and subsequently every other day, until day 17. Cell viability and oxidative stress experiments performed with the 96-well plate co-cultures were initiated on day 17.

Exposure of transwell tri-culture and 96-well plate cocultures to digesta. The transwell inserts and 96-well plates were rinsed with glucose-free DMEM supplemented with 10 mM HEPES buffer, 100 IU mL^{-1} penicillin, 100 μg mL^{-1} streptomycin and non-essential amino acids (1/100 dilution of 100× solution, ThermoFisher), 10 mM pyruvate (ThermoFisher). The final small intestinal digesta from simulated digestions were combined with glucose-free DMEM media in a ratio of 1 : 3, and the mixture was applied to the cells (1.5 ml to the apical compartment for transwell inserts, 200 μl per well for 96-well plates). Apical fluid in untreated control wells was replaced with fresh glucose-free media. Digesta was also dispensed in a cell-free control well. Transwell cells were incubated with digesta for 4 h. At the end of exposure, TEER in transwells was measured as described above, and supernatants from transwells were collected for LDH analysis. Assessment of ROS production and cell viability (described below) was performed after 4 h exposures, respectively, in 96-well plates.

***In vitro* maltose and glucose translocation across the small intestinal epithelium.** Biokinetics of maltose and glucose from small intestinal phase digestas was assessed using the tri-culture model of the small intestinal epithelium grown on transwell inserts. Unlike typical glucose uptake/transport studies that employ fluorescent and radiolabeled glucose analogs,[68–70] since the glucose in our studies is derived from maltose released from starch, and cannot be labeled, it was necessary to measure uptake and transport of free maltose and glucose using a fluorometric assay. This in turn required the use of glucose-free cell culture media during the experiments to sufficiently reduce background glucose signal to allow accurate measurement of glucose transport. Glucose-free DMEM without serum was therefore used in this study. However, in an initial pilot studies cells were adversely affected by the absence of glucose, with significant loss of tight junction integrity and viability within a few hours without a glucose source (data not shown), and therefore pyruvate, the end product of glycolysis, was added to the glucose-free media as a replacement energy source.[71,72] One glucose molecule yields the equivalent of 5 ATP during glycolysis to yield 2 molecules of pyruvate. Each molecule of pyruvate produces the equivalent of 12.5 ATP through oxidative decarboxylation and the reactions of the Krebs cycle.[73] Thus exogenous pyruvate should provide an adequate replacement energy source for cells deprived of glucose.

Several concentrations of pyruvate (from 1 to 20 mM, *i.e.*, 1× to 20× concentrations normally used in cell culture) were tested to identify the optimal supplementation concentration during 4 h biokinetics experiment exposures. The results of these optimization experiments are shown in Fig. S1.† After 4 hours exposure to glucose-free medium with pyruvate, cell layer integrity was assessed by measuring trans-epithelial electrical resistance (TEER), cell injury and death were assessed by measuring lactate dehydrogenase (LDH) release, and oxidative stress was assessed by measuring reactive oxygen species (ROS) production, as described below. Based on these optimization study results a pyruvate concentration of 10 mM was selected for the glucose uptake and biokinetics experiments.

Biokinetic experiments were performed on day 17. After loading the mixtures of digesta and glucose-free medium, 150 μL fluids from apical and basolateral chambers were collected at the time points of 0.5, 1.0, 2.0, 4.0 hours. The amount of maltose/glucose in digesta or medium was assessed using the maltose and glucose assay kit (Sigma-Aldrich) according to the manufacturer's instructions. Maltose is converted to two glucose units *via* α-D-glucosidase, and glucose is then oxidized, resulting in a fluorometric (λ_{ex} = 535, λ_{em} = 587 nm) product, proportional to the maltose present. Each sample was measured both with and without α-D-glucosidase to differentiate between maltose and free glucose.

To evaluate effects of the ENMs on the biokinetics of glucose in the absence of starch (*e.g.*, from high fructose corn syrup or honey), we measured total glucose in the basolateral and apical fluids of transwell tri-cultures over time as described above after application to the apical compartment of small intestinal digestas of water with or without test materials at 1% w/w (but without starch) spiked with glucose at a concentration equivalent to complete digestion of a 1% initial starch suspension.

Glucose absorbed by cells (removed from the apical compartment) at each time point were calculated by subtracting the total apical glucose at that time from the starting total apical glucose mass. Glucose either stored or used by cells was calculated at each time point by subtracting

 This journal is © The Royal Society of Chemistry 2021

Published on 20 July 2021. Downloaded by Fail Open on 7/23/2025 9:11:29 AM.

both total apical and basolateral glucose from the initial total apical glucose.

Cytotoxicity (lactate dehydrogenase (LDH) release). Cytotoxicity was assessed using a triculture model of the small intestinal epithelium grown on transwell inserts or in 96-well plates.[49] Supernatants from transwells were collected after 24 h exposures for LDH analysis, which was performed using the Pierce LDH assay kit (Sigma Aldrich) according to manufacturer's instructions. Untreated control wells were used to measure spontaneous LDH release. For maximum LDH release control wells, 150 μL of apical fluid was removed and replaced with 150 μL 10× lysis buffer 45 minutes prior to the end of incubation. The provided substrate was dissolved in 11.4 mL of ultrapure water and added to 0.6 mL assay buffer to prepare the reaction mixture. Apical fluid in each well was pipetted to the mix and 150 μL was transferred to a 1.5 mL tube. Tubes were centrifuged at 5000 × *g* for 5 min, and 50 μL of the supernatant from each tube was dispensed in triplicate wells in a fresh 96-well plate. 50 μL of reaction mixture was added and mixed by tapping the plate. Plates were incubated at room temperature for 30 minutes or less (to provide maximum difference in color between samples by visual inspection), and 50 mL stop solution was added and mixed by tapping. Absorbance was measured at 490 nm (A_{490}) and 680 nm (A_{680}). To calculate LDH activity, A_{680} values were subtracted from measured A_{490} values to correct for instrument background. To correct for digesta background, LDH activities from no-cell controls were subtracted from test well LDH activities. Percent cytotoxicity was calculated by subtracting spontaneous LDH release values from treatment values, dividing by total LDH activity (maximum LDH activity – spontaneous LDH activity), and multiplying by 100.

Cell viability (mitochondrial metabolic activity). Cell viability was assessed using the PrestoBlue™ reagent (Thermo Fisher Scientific, Inc., Waltham, MA, Cat, no. A13261). PrestoBlue is a soluble tetrazolium salt that readily enters cells, where it is reduced, in metabolically active (viable) cells, by mitochondrial dehydrogenases and reductases, to an insoluble, blue-colored, red-fluorescent formazan product. The PrestoBlue™ viability assay was performed after 24 h exposure to digestas, using 96-well plate co-cultures, according to manufacturer's instructions. Briefly, cells were washed 3 times with 200 μL per well PBS, and 100 μL of 10% PrestoBlue reagent was added to each well. Plates were then incubated at 37 °C for 15 minutes, and fluorescence was measured at 560 nm (excitation)/590 nm (emission).

Oxidative stress (ROS production). Oxidative stress was assessed by measuring cellular ROS accumulation after 6 h exposure to digestas in 96-well co-cultures. ROS production (oxidative stress) was assessed using the CellROX® green reagent (Thermo Fisher Scientific, Inc.) according to the manufacturer's instructions. Briefly, a 5 mM working solution of the CellROX® green reagent was prepared from 20 mM stock by diluting in glucose-free DMEM media without FBS. Media was removed from test wells and replaced with 100 μL of working solution, and plates were incubated for 30 minutes at 37 °C. Cells were then washed 3 times with 200 μL per well PBS, and fluorescence was measured at 480 nm (excitation)/520 nm (emission).

Statistical analysis. Statistical analysis and preparation of graphs was performed using Prism 9.02 software (GraphPad Software, Inc.). Comparison of groups for all measurements were performed by one-way ANOVA with Dunnett's multiple comparisons test.

Results

Characterization of cellulose and chitosan nanomaterials

Extensive characterization of the cellulose nanocrystals (CNC) and cellulose nanofibrils (CNF) used in these studies has been performed and the results previously published by the authors.[62,74] Physical and morphological characterization, including transmission and cryo-scanning electron microscopy (TEM and Cryo-SEM), and chemical analysis, including inductively coupled plasma mass spectrometry (ICP-MS), X-ray photoelectron spectroscopy (XPS), and infrared spectroscopy (IR) of pristine as synthesized CNC and CNF were reported by Pyrgiotakis *et al.*[62] Colloidal characterization of CNC and CNF suspended in deionized water and culture media by field emission SEM (FE-SEM) was reported, along with optimization of dispersion methods and *in vitro* and particle kinetics of FITC-labeled CNF in media, by Bitounis *et al.*[74] Detailed characterization of the chitosan nanoparticles (Chnp) used in these studies was also performed and previously published. Physical and morphological characterization of pristine Chnp was reported along with the details of its synthesis by Sampathkumar *et al.*[63] Colloidal characterization of Chnp dispersions in water and transformations of Chnp across the GI tract during digestion were reported by Guo *et al.*[48]

Key property values from these previous studies are shown, along with zeta potentials for CNF and CNC materials, which were measured for this study, in Table S1.† CNC comprised long needle shaped particles with an average size of 270 ± 90 × 25 ± 9 nm and an average aspect ratio of 11.5 ± 3.2. CNF consisted of highly branched, complex, and variable agglomerates averaging 6710 ± 5611 × 64 ± 29 nm in size with an aspect ratio of 107.6 ± 54.5. Chitosan nanoparticles were roughly spherical, as observed by SEM, with an average diameter by BET of 159.8 ± 2.3 nm and an average hydrodynamic diameter of 175.8 ± 37.4 nm by DLS.[63] It should be noted that although determination of hydrodynamic diameter by DLS is useful for roughly spherical engineered nanomaterials (ENMs) such as Chnp, because of the large aspect ratios of both CNC and CNF, and the highly branched and complex structure of CNF in particular, an accurate and meaningful measurement of hydrodynamic diameter by DLS is not possible for those materials.

The zeta potential of Chnp in water was +20.8 ± 3.01 mV.[63] In contrast, both cellulose materials had negative zeta potentials. Specifically, CNF had a moderately negative zeta potential of −7.43 ± 3.25 mV and CNC had a more strongly

Published on 20 July 2021. Downloaded by Fail Open on 7/23/2025 9:11:29 AM.

negative zeta potential of −27.4 ± 1.21 mV. These zeta potentials are consistent with the known surface chemistry of these materials and the pK_αs of the respective corresponding primary amine (Chnp), hydroxyl (CNF), and sulfate ester (CNC, produced by sulfuric hydrolysis) groups.

Effects of cellulose and chitosan nanomaterials on starch digestion

To evaluate possible effects on the enzymatic hydrolysis and release of maltose (glucose dimers), we measured free maltose and glucose and calculated the percentage of the initial starch digested during simulated digestion of gelatinized starch suspensions with or without test materials as described in the method section above. Results of these studies are summarized in Fig. 2. At an initial concentration of 1% w/w in 1% gelatinized rice starch suspensions, CNF caused a slight but significant decrease (11%, $p < 0.05$) in percent starch digested relative to starch only controls. Chnp, in contrast, caused a slight but significant increase (14%, $p < 0.01$) in percent starch digested, whereas CNC had no significant effect (Fig. 2a). CNC also had no effect on digestion of 1% w/w gelatinized rice starch at either lower or higher CNC concentrations (Fig. 2b). Similarly, CNC had no significant effect on digestion of 1% corn or wheat starch suspensions at 2% w/w starting food model concentration (Fig. 2c). Finally, neither CNF nor CNC at 2% w/w food concentration significantly modulated digestion of rice starch at a concentration of 5% (Fig. 2d).

Effects of cellulose and chitosan nanomaterials on absorption of glucose from digested starch

To evaluate possible effects of the test ENMs on the biokinetics of glucose absorption from digested starch, we measured total glucose in the basolateral and apical fluids of transwell intestinal epithelial tri-cultures over time after application of small intestinal digestas of 1% rice starch suspensions with or without test ENMs at 1% w/w starting food model concentrations to the apical compartments. The results of these studies are summarized in Fig. 3. Slight differences were seen in the apical and basolateral compartment glucose curves (Fig. 3a and c) and the calculated glucose uptake (glucose removed from the apical compartment) curves (Fig. 3b). Most notably, apical glucose was greater initially and at all subsequent time points in samples containing Chnp, consistent with the slight increase in starch digestion in the presence of Chnp noted above. Area under the curve (AUC) calculations of the basolateral glucose curves, which represent an estimate of epithelial glucose translocation or physiological absorption (analogous to the incremental area under the curve (iAUC) of postprandial serum glucose used to determine the

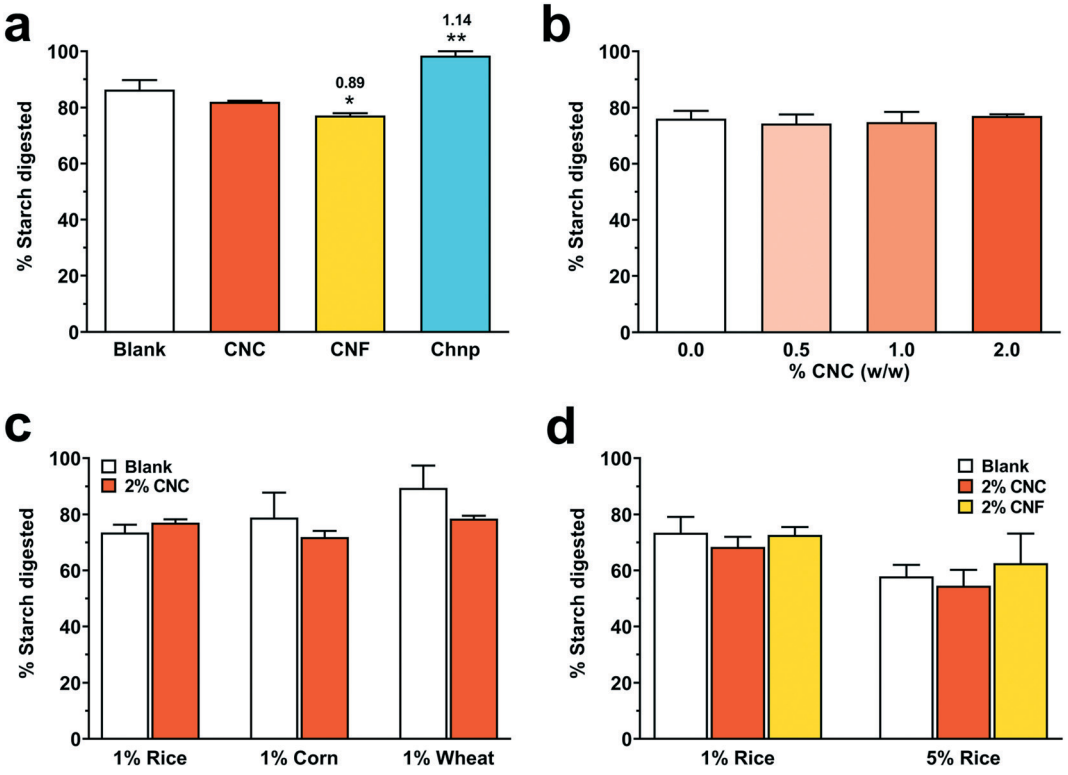

Fig. 2 Effects of cellulose and chitosan nanomaterials on digestion of starch. Percent total starch digested in the presence of ENMs a. percent starch digested from initial 1% rice starch suspensions containing 1% ENM, b. percent starch digested from initial 1% rice starch suspensions containing CNC at varied concentrations. c. Percent starch digested from different types of starch at 1% with and without 2% CNC d. percent starch digested from 1% or 5% rice starch suspensions with and without 2% CNC or CNF. Error bars represent one standard deviation. Numbers above bars represent fold change relative to blank. *$p < 0.05$, **$p < 0.01$.

 This journal is © The Royal Society of Chemistry 2021

Published on 20 July 2021. Downloaded by Fail Open on 7/23/2025 9:11:29 AM.

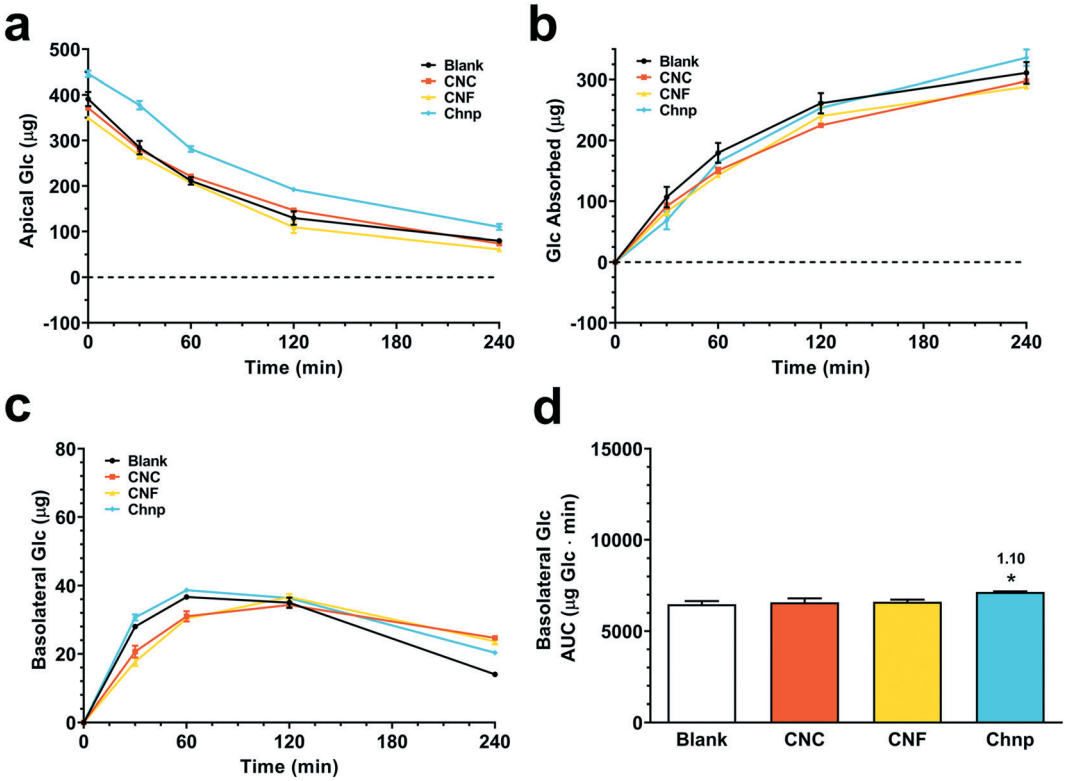

Fig. 3 Effects of cellulose and chitosan nanomaterials on absorption of glucose from starch. a. Apical chamber glucose concentration over time, b. total absorbed glucose over time c. basolateral glucose concentration over time. d. AUC of basolateral concentration curves. Error bars represent one standard deviation. Numbers above bars represent fold change relative to blank. *$p < 0.05$.

glycemic index of foods) revealed only a slight (10%, $p < 0.5$) increase in glucose absorption in the presence of Chnp (Fig. 3d), consistent with greater substrate availability as a result of the greater apical glucose mass and thus concentration in the presence of Chnp. None of the other materials had any significant effects within the 4 hours time of exposure. The calculated glucose utilization and translocation rate curves showed some variation among treatments but were not particularly revealing (Fig. S2†).

It should be noted that at the time that digestas from starch solutions were applied to cells, after storage of digestas at 4 °C for 48 h, 90% of the glucose present was in the form of maltose (Fig. S3†). Immediately following digestion, maltose accounts for 100% of total glucose. However, while we can find no previous account of this in the literature, maltose apparently undergoes spontaneous hydrolysis to glucose at a fairly brisk rate, with 75% hydrolyzed in 41 days. Moreover, this rate may depend on the presence of ENMs. Because of this, it was not possible to analyze maltose and glucose contributions to total glucose in the apical chambers over time, since the samples had been stored for up to 3–4 weeks prior to analysis.

Effects of cellulose and chitosan nanomaterials on absorption of glucose from digestas spiked with glucose

In order to isolate potential effects of the test materials on glucose absorption, and because processed foods often include free glucose *via* added corn syrup or other sweeteners, we studied the absorbance of glucose alone (*i.e.*, digestas of water spiked with glucose). Differences in the apical compartment glucose and glucose uptake curves (Fig. 4a and b) suggest that the presence of each of the test ENMs may have reduced the rate of glucose uptake by the epithelium. However, the basolateral compartment glucose (representing translocation and physiological absorption) curves (Fig. 4c), and basolateral glucose AUC values (analogous to glycemic index) calculated from them (Fig. 4d) showed substantial and highly significant increases in glucose translocation in the presence of any of the ENMs (increases in AUC relative to blank controls of 20%, $p < 0.01$ for CNC, 49%, $p < 0.001$ for CNF, and 60%, $p < 0.001$ for Chnp). Since glucose cannot leave the system, the apparent disparity between reduced total uptake and increased translocation in the presence of these materials must be due to differences in glucose utilization by the cells (*i.e.*, cells exposed to the test ENMs store or metabolize less glucose that control treatment cells). Calculated glucose utilization and translocation rate curves (Fig. S4†) illustrate this decreased utilization.

In vitro toxicity of cellulose and chitosan nanomaterials in a starchy food matrix

To assess the potential cytotoxicity of the test materials in the presence of starch and thereby rule out the possibility that direct cytotoxicity may have contributed to the observed effects,

Published on 20 July 2021. Downloaded by Fail Open on 7/23/2025 9:11:29 AM.

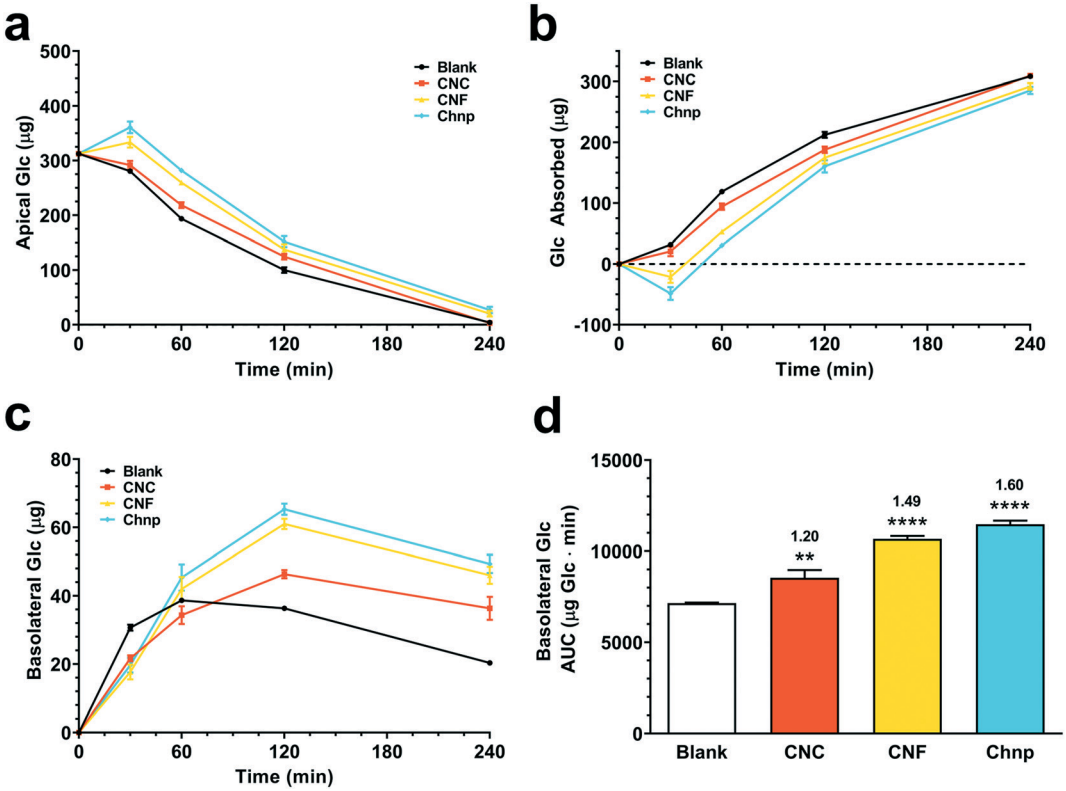

Fig. 4 Effects of cellulose and chitosan nanomaterials on absorption of glucose from digestas spiked with glucose. a. Apical chamber glucose concentration over time, b. total absorbed glucose over time c. basolateral glucose concentration over time. d. AUC of basolateral concentration curves. Error bars represent one standard deviation. Numbers above bars represent fold change relative to blank. $^{**}p < 0.01$, $^{****}p < 0.001$.

changes in transepithelial electrical resistance (TEER), cytotoxicity (LDH release), cell viability, and reactive oxygen species (ROS) generation in tri-culture cells after exposure to digestas of the test ENMs in water with or without 1% rice starch were assessed as described in method section above. The results of these studies are summarized in Fig. 5. None of the test materials, either with or without starch, had any significant effects on TEER (Fig. 5a), cytotoxicity (Fig. 5b), cell viability (Fig. 5c), or ROS generation (Fig. 5d).

Discussion and conclusions

Although none of the materials tested had a very sizeable effect on starch digestion, some effects and notable differences between the effects of the different materials tested were observed. Specifically CNF caused a slight (11%, $p < 0.05$) decrease, while Chnp caused a modest increase (14%, $p < 0.01$), and CNC had no effect, on starch digestion. Although further studies would be needed to uncover the specific mechanisms responsible for these differences, one could speculate that the differences in surface chemistries among these three materials might play a role. Specifically, the predominant surface functional group of CNF is the hydroxyl group of its glucose monomers, which would remain protonated and uncharged under all physiological conditions, and participate in hydrogen bonding that stabilizes interactions between adjacent glucose chains. Chnp, in addition to having many hydroxyl groups, is decorated with the primary amine groups of its deacetylated glucosamine monomers, which have a pK_a of about 6.5, and are thus protonated and positively charged in the acidic conditions of the stomach (or gastric phase of digestion) but largely deprotonated and uncharged at neutral pH (*i.e.*, in the food model, oral phase, and small intestinal phase). CNC, on the other hand, being produced by acid hydrolysis, typically with sulfuric acid, has on its surface (in addition to hydroxyl groups) a number of acidic sulfate groups, which would be negatively charged throughout digestion. In addition to disrupting the hydrogen bonding of a continuous field of hydroxyl groups, the presence of charged functional groups could conceivably alter interactions of the biopolymers with either the starch glucose monomer chains or with α-amylase. A better understanding of the role of charged or other functional groups in modulation of starch digestion could be gained by studying the effects of a specifically engineered chemically modified variants of biopolymer nanomaterials.

In addition, whereas 1% CNF slightly decreased digestions of starch in a 1% starch food model, no effect was observed with 2% CNF (with either 1% or 5% starch). This apparent discrepancy may indicate that the observed reduction at 1% starch is not significant, or may be due to differences in the physical or chemical properties between a 1% and 2% CNF suspension. A 2% CNF suspension is noticeably and considerably more viscous than a 1% solution, which one

 This journal is © The Royal Society of Chemistry 2021

Published on 20 July 2021. Downloaded by Fail Open on 7/23/2025 9:11:29 AM.

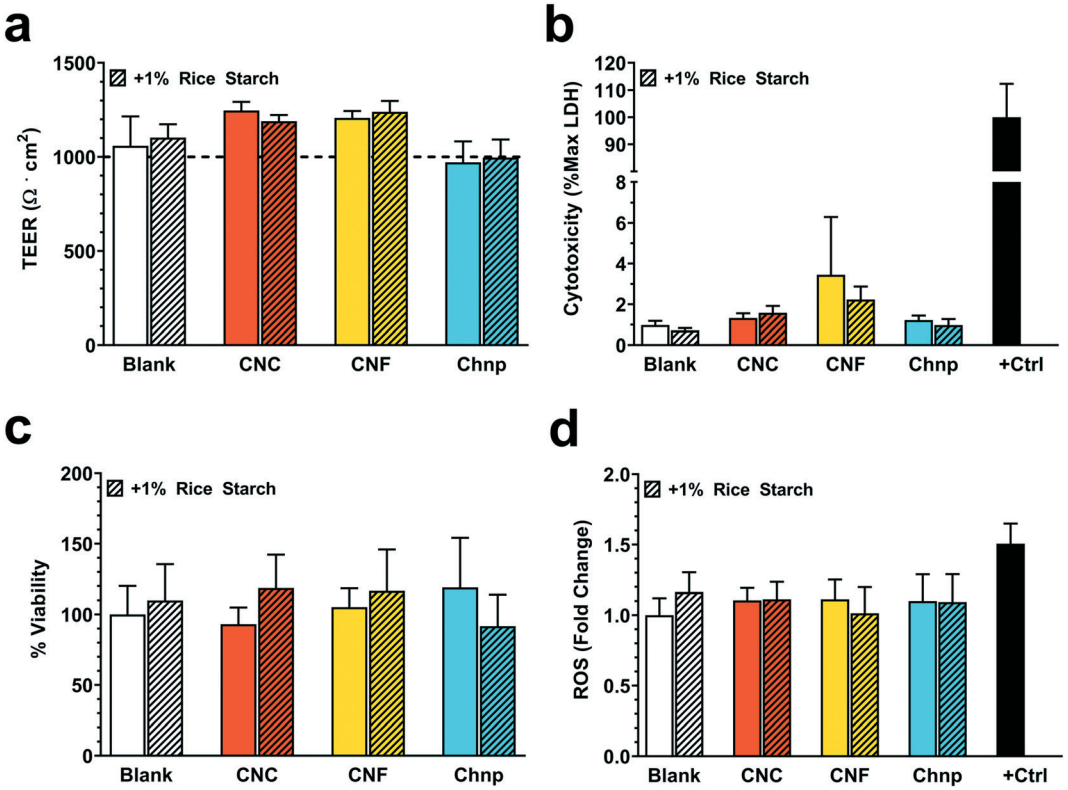

Fig. 5 Toxicological studies of ingested cellulose and chitosan nanomaterials with and without starch. a. TEER, b. LDH c. viability. d. ROS generation.

might expect to reduce mobility of α-amylase and its amylose or amylopectin substrate and thereby reduce digestion. Our results, however, indicate the opposite – that the higher concentration somehow restores the reduction of activity that occurred at the lower concentration. One possibility is that at the higher concentration a greater portion of the CNF chains and proportion of their surface areas are interacting with other CNF chains or monomers (*e.g.*, *via* hydrogen bonding) which may limit the effective area or number surface hydroxyl groups available for the kind of interactions with the substrate or other biomolecules that caused the reduction of starch digestion at the lower concentration.

Nevertheless, the slight (11%) but significant decrease in digestion of starch seen at 1% CNF is consistent with findings previously reported by Liu *et al.*,[59] and thus further supports the idea that CNF could potentially have a hypoglycemic or glycemia dampening effect when added to starch-containing foods.

Whereas effects on starch digestion were relatively small (Fig. 2), and absorption from maltose (digested starch) was unaffected (Fig. 3), all three materials caused a substantial and significant increase in translocation (absorption) of free glucose (from digestion of glucose alone) at the same mass concentration (Fig. 4). The AUC values calculated from the *in vitro* transwell model in this study are analogous to the incremental area under the curve (iAUC) values used to represent the glycemic index of foods, which are calculated from postprandial serum glucose measurements in human subjects. Since significant oral exposures to cellulose and chitosan nanomaterials like those investigated here would result from many of the applications for which they are being considered, particularly their use in foods as stabilizers or emulsifiers, the potential to increase absorption of co-ingested glucose (*e.g.*, from corn syrup or honey) suggested by our findings could be problematic and deserve further study.

Additional studies are required to elucidate the mechanism(s) underlying the observed increases in glucose translocation in the presence of CNF, CNC, and Chnp, and importantly to attempt to explain why the ENMs impacted translocation of free glucose (Fig. 4) but not of maltose at the same mass concentration (Fig. 3). It is possible that the rate-limiting step, at the concentrations employed in these studies, for glucose absorption from maltose is the cleavage of maltose by enterocyte brush border maltase to form glucose, and that at the presumably lower concentrations of glucose produced by this activity the ENMs have no effect. Potential mechanisms for the observed effects on free glucose absorption, which are summarized in Fig. S5,† include: 1) reduced viscosity and increased diffusion of glucose within intestinal mucus or luminal fluid (small intestinal digesta); 2) increased paracellular transport due to changes in cellular junctions; and 3) increased number or activity of enterocyte glucose transporters, including the sodium/glucose co-transporter, SGLT1, which mediates most of the glucose uptake at low to moderate luminal glucose concentrations (<~20 mM),[75–77] and glucose transporter type 2 (GLUT2),

Published on 20 July 2021. Downloaded by Fail Open on 7/23/2025 9:11:29 AM.

which is believed to provide high capacity apical uptake *via* facilitated transport at high luminal glucose concentrations (>20 mM), as well as exit of glucose at the basolateral membrane,[75–77] although the role of GLUT2 in uptake remains controversial.[78] Examination of the rheological properties (viscosity, sheer rate) of small intestinal digestas and artificial mucus exposed to digestas, and of the diffusion rate of glucose in digestas and mucus will allow us to assess the role of such changes in the observed effects. The role of paracellular transport can be assessed by measuring glucose translocation in the presence of inhibitors for both SGLT1 and GLUT2 (*e.g.*, phlorizin and phloretin, respectively), which should eliminate all but diffusive or paracellular transport. The relative contributions of the two transporters can be assessed using single inhibitor treatments to disable either SGLT1 (phlorizin) or GLUT2 (phloretin) to isolate the effects of the other transporter.

Preformed GLUT2 transporters are thought to be trafficked in endosomal vesicles and inserted into the apical membrane in response to increasing apical glucose concentrations and uptake.[77] Uptake of sodium and glucose by SGLT1 causes a slight membrane depolarization, which is thought to activate apical voltage-gated calcium channels (Ca_v 1.3), which results in calcium influx and cytoskeletal changes that enable the protein trafficking and signaling that lead to GLUT2 insertion. The enterocyte apical taste receptor T1R2/3 is also believed to play a role by activating cytoplasmic phospholipase C β2 (PLC β2) and protein kinase C (PKC) and thereby initiating signaling *via* PIP2/IP3 that culminates in trafficking of GLUT2-containing endosomes to and insertion of GLUT2 transporters in the apical membrane. If we find, based on single inhibitor studies alluded to above, that GLUT2 plays a role in the observed effects of CNF, CNC, and Chnp on glucose transport, it may be possible to observe insertion of GLUT2 in the apical membranes by immunostaining and confocal microscopy. The roles of Ca_v 1.3 calcium channels, T1R2/3 taste receptors, PLC, and PKC can then be assessed using specific inhibitors for each target (nifedipine for Ca_v 1.3, lactisole for T1R2/3, U-73112 for PLC, and BIM-1 for PKC) for Ca_v 1.3 channel, the roles of calcium channels.

It should be noted that the concentration of starch and glucose used in these studies, at an initial food concentration of 1% by weight (corresponding to ~0.2 mM applied in the final digesta to the tri-culture cells after ~1/12 dilution during the digestion process and an additional 1/4 dilution of the final digesta in culture medium required to maintain tri-culture cell health during exposures), are relatively low compared to those that might be present in a high sugar or starch meal. However, it is not considerably lower than that present in a standardized food model based on the American diet, which recently developed by our lab,[50] in which the total carbohydrate concentration is ~1.8% w/w (which would correspond to ~0.36 mM applied to tri-culture cells). Even a pure starch meal (*e.g.*, pasta) typically contains <20% total carbohydrates, which would result in a ~0.72 mM total carbohydrate concentration applied to cells in our system. Nevertheless, it is important to consider the influence that concentration may have in such studies, particularly since the aforementioned insertion of GLUT2 and subsequent GLUT2 transport is thought to be concentration dependent, and not to occur to an appreciable extent at glucose concentrations of less than ~20 nM in the intestinal lumen.[77]

It is interesting that while all three test nanomaterials significantly increased glucose absorption, the magnitude of the effect was substantially greater for CNF, and particularly for Chnp, than for CNC. Since, as discussed above, these three materials have distinctly different surface chemistries, we might speculate that surface functional groups play an important role. Since CNC bears negatively charged sulfate groups[63] under all conditions and had a much smaller effect than the other materials, and because Chnp, which may carry partially protonated and positively charged amino groups at neutral pH,[27,48,63,79,80] had the largest effect, we might further speculate that the biopolymer nanomaterial – nutrient, biomolecule, or cell interactions responsible for the observed effect on glucose translocation are favored by positively charged groups, and may involve interactions with anionic protein residues or other biomolecules. An understanding of the mechanism underlying the observed effects may help to explain these differences. As with the effects of surface chemistry on starch digestion, future studies with specifically engineered chemically modified variants of biopolymer nanomaterials may help to explain the observed differences in the effects of these materials on intestinal glucose translocation.

Together the findings reported here suggest that cellulose and chitosan biopolymer ENMs, which are being considered as potential food additives and excipients for nutrient supplements and drugs by the respective industries, may substantially increase the bioavailability of dietary glucose, which would in turn substantially increase the effective glycemic index of foods containing corn syrup, honey, or other direct sources of glucose. Even a small increase in the glycemic index of common processed foods (which often simultaneously contain both corn syrup and a thickening or emulsifying ingredient) that are consumed by millions of people could have important individual and public health implications in an obese population with a high prevalence of diabetes and prediabetes.

As noted above, previous feeding studies in rats found that CNF had no effect on blood glucose,[60] and a subchronic gavage study in mice revealed altered glucose homeostasis and a slight reduction in lean body weight,[61] but neither of these subchronic studies either confirmed or ruled out potential acute hypoglycemic or hyperglycemic effects, which may be missed if sampling does not immediately follow feeding (*i.e.*, postprandial glucose), or include measurement of persistent markers of glycemia upper excursions (*e.g.*, HbA1c). Moreover these previous studies did not examine the effects of CNF on the absorption of dietary glucose. Further studies are needed to examine the effects of CNF on blood glucose levels and AUCs immediately after high glucose

 This journal is © The Royal Society of Chemistry 2021

Published on 20 July 2021. Downloaded by Fail Open on 7/23/2025 9:11:29 AM.

feeding. If a hyperglycemic effect is confirmed then additional studies will be needed to identify the mechanism or mechanisms responsible.

Conflicts of interest

There are no conflicts to declare.

Acknowledgements

Support for the research reported, including assets and resources required for designing and performing experiments, data analysis, and interpretation, was provided by the Nanyang Technological University-Harvard T. H. Chan School of Public Health Initiative for Sustainable Nanotechnology. Research reported in this publication was supported by the HSPH Center for Nanotechnology and Nanotoxicology and National Institute of Environmental Health Sciences of the National Institutes of Health under Award Number (NIH grant # U24ES026946) as part of the Nanotechnology Health Implications Research (NHIR) Consortium, and the NIEHS Environmental Health Center Grant (#ES-000002). The content is solely the responsibility of the authors and does not necessarily represent the official views of the National Institutes of Health.

The engineered nanomaterials used in the research presented in this publication were developed, characterized, and provided by the Engineered Nanomaterials Resource and Coordination Core established at Harvard T. H. Chan School of Public Health (NIH grant # U24ES026946) as part of the Nanotechnology Health Implications Research Consortium.

References

1 O. Riccio, M. E. van Gijn, A. C. Bezdek, L. Pellegrinet, J. H. van Es, U. Zimber-Strobl, L. J. Strobl, T. Honjo, H. Clevers and F. Radtke, Loss of intestinal crypt progenitor cells owing to inactivation of both Notch1 and Notch2 is accompanied by derepression of CDK inhibitors p27 ^{Kip1} and p57 ^{Kip2}, *EMBO Rep.*, 2008, **9**, 377–383.

2 A. Pinna, L. Malfatti, G. Galleri, R. Manetti, S. Cossu, G. Rocchitta, R. Migheli, P. A. Serra and P. Innocenzi, Ceria nanoparticles for the treatment of Parkinson-like diseases induced by chronic manganese intoxication, *RSC Adv.*, 2015, **5**, 20432–20439.

3 T. Xu, C. Ma, Z. Aytac, X. Hu, K. W. Ng, J. C. White and P. Demokritou, Enhancing agrichemical delivery and seedling development with biodegradable, tunable, biopolymer-based nanofiber seed coatings, *ACS Sustainable Chem. Eng.*, 2020, **8**(25), 9537–9548.

4 K. Mattsson, E. V. Johnson, A. Malmendal, S. Linse, L. A. Hansson and T. Cedervall, Brain damage and behavioural disorders in fish induced by plastic nanoparticles delivered through the food chain, *Sci. Rep.*, 2017, **7**, 1–7.

5 J. Matricon, M. Meleine, A. Gelot, T. Piche, M. Dapoigny, E. Muller and D. Ardid, Review article: associations between immune activation, intestinal permeability and the irritable bowel syndrome, *Aliment. Pharmacol. Ther.*, 2012, **36**, 1009–1031.

6 W. Luu, D. Bousfield and J. Kettle, in *Proc. Technical Association of Pulp and Paper, PaperCon symposium*, 2011, pp. 2222–2233.

7 S. Kabiri, F. Degryse, D. N. H. Tran, R. C. da Silva, M. J. McLaughlin and D. Losic, Graphene Oxide: A New Carrier for Slow Release of Plant Micronutrients, *ACS Appl. Mater. Interfaces*, 2017, **9**, 43325–43335.

8 M. Camilleri and H. Gorman, Intestinal permeability and irritable bowel syndrome, *Neurogastroenterol. Motil.*, 2007, **19**, 545–552.

9 L. Armand, M. Biola-Clier, L. Bobyk, V. Collin-Faure, H. Diemer, J.-M. Strub, S. Cianferani, A. Van Dorsselaer, N. Herlin-Boime, T. Rabilloud and M. Carriere, Molecular responses of alveolar epithelial A549 cells to chronic exposure to titanium dioxide nanoparticles: A proteomic view, *J. Proteomics*, 2016, **134**, 163–173.

10 F. Araújo and B. Sarmento, Towards the characterization of an in vitro triple co-culture intestine cell model for permeability studies, *Int. J. Pharm.*, 2013, **458**, 128–134.

11 R. A. Khan, S. Salmieri, D. Dussault, J. Uribe-Calderon, M. R. Kamal, A. Safrany and M. Lacroix, Production and properties of nanocellulose-reinforced methylcellulose-based biodegradable films, *J. Agric. Food Chem.*, 2010, **58**, 7878–7885.

12 M. Mariano, N. El Kissi and A. Dufresne, Cellulose nanocrystals and related nanocomposites: Review of some properties and challenges, *J. Polym. Sci., Part B: Polym. Phys.*, 2014, **52**, 791–806.

13 S. S. Nair, J. Zhu, Y. Deng and A. J. Ragauskas, High performance green barriers based on nanocellulose, *Sustainable Chem. Processes*, 2014, **2**, 23.

14 K. J. Ong, J. A. Shatkin, K. Nelson, J. D. Ede and T. Tetsina, Establishing the safety of novel bio-based cellulose nanomaterials for commercialization, *NanoImpact*, 2017, **6**, 19–29.

15 G. Strom, C. OHgren and M. Ankerfors, *Nanocellulose as an additive in foodstuff*, Stockholm, Sweden, 2013.

16 I. Shahabi-Ghahfarrokhi, F. Khodaiyan, M. Mousavi and H. Yousefi, Green bionanocomposite based on kefiran and cellulose nanocrystals produced from beer industrial residues, *Int. J. Biol. Macromol.*, 2015, **77**, 85–91.

17 G. M. Deloid, I. S. Sohal, L. R. Lorente, R. M. Molina, G. Pyrgiotakis, A. Stevanovic, R. Zhang, D. J. McClements, N. K. Geitner, D. W. Bousfield, K. W. Ng, S. C. J. Loo, D. C. Bell, J. Brain and P. Demokritou, Reducing Intestinal Digestion and Absorption of Fat Using a Nature-Derived Biopolymer: Interference of Triglyceride Hydrolysis by Nanocellulose, *ACS Nano*, 2018, **12**, 6469–6479.

18 L. M. Ensign, C. Schneider, J. S. Suk, R. Cone and J. Hanes, Mucus penetrating nanoparticles: biophysical tool and method of drug and gene delivery, *Adv. Mater.*, 2012, **24**, 3887–3894.

19 M. Mohammed, J. Syeda, K. Wasan and E. Wasan, An Overview of Chitosan Nanoparticles and Its Application in Non-Parenteral Drug Delivery, *Pharmaceutics*, 2017, **9**, 53.

Published on 20 July 2021. Downloaded by Fail Open on 7/23/2025 9:11:29 AM.

20 A. Dube, J. A. Nicolazzo and I. Larson, Chitosan nanoparticles enhance the intestinal absorption of the green tea catechins (+)-catechin and (−)-epigallocatechin gallate, *Eur. J. Pharm. Sci.*, 2010, **41**, 219–225.

21 C. Feng, Z. Wang, C. Jiang, M. Kong, X. Zhou, Y. Li, X. Cheng and X. Chen, Chitosan/o-carboxymethyl chitosan nanoparticles for efficient and safe oral anticancer drug delivery: In vitro and in vivo evaluation, *Int. J. Pharm.*, 2013, **457**, 158–167.

22 M. Diop, N. Auberval, A. Viciglio, A. Langlois, W. Bietiger, C. Mura, C. Peronet, A. Bekel, D. Julien David, M. Zhao, M. Pinget, N. Jeandidier, C. Vauthier, E. Marchioni, Y. Frere and S. Sigrist, Design, characterisation, and bioefficiency of insulin–chitosan nanoparticles after stabilisation by freeze-drying or cross-linking, *Int. J. Pharm.*, 2015, **491**, 402–408.

23 L. Yin, J. Ding, C. He, L. Cui, C. Tang and C. Yin, Drug permeability and mucoadhesion properties of thiolated trimethyl chitosan nanoparticles in oral insulin delivery, *Biomaterials*, 2009, **30**, 5691–5700.

24 A. Sadeghi, F. Dorkoosh, M. Avadi, M. Weinhold, A. Bayat, F. Delie, R. Gurny, B. Larijani, M. Rafieetehrani and H. Junginger, Permeation enhancer effect of chitosan and chitosan derivatives: Comparison of formulations as soluble polymers and nanoparticulate systems on insulin absorption in Caco-2 cells, *Eur. J. Pharm. Biopharm.*, 2008, **70**, 270–278.

25 Z. Ma and L.-Y. Lim, Uptake of Chitosan and Associated Insulin in Caco-2 Cell Monolayers: A Comparison Between Chitosan Molecules and Chitosan Nanoparticles, *Pharm. Res.*, 2003, **20**, 1812–1819.

26 F. Cui, F. Qian, Z. Zhao, L. Yin, C. Tang and C. Yin, Preparation, Characterization, and Oral Delivery of Insulin Loaded Carboxylated Chitosan Grafted Poly(methyl methacrylate) Nanoparticles, *Biomacromolecules*, 2009, **10**, 1253–1258.

27 K. Sampathkumar, S. Riyajan, C. K. Tan, P. Demokritou, N. Chudapongse and S. C. J. Loo, Small-Intestine-Specific Delivery of Antidiabetic Extracts from Withania coagulans Using Polysaccharide-Based Enteric-Coated Nanoparticles, *ACS Omega*, 2019, **4**, 12049–12057.

28 R. A. Yokel, S. Hussain, S. Garantziotis, P. Demokritou, V. Castranova and F. R. Cassee, The Yin: An adverse health perspective of nanoceria: uptake, distribution, accumulation, and mechanisms of its toxicity, *Environ. Sci.: Nano*, 2014, **1**, 406–428.

29 J. D. Sisler, S. V. Pirela, J. Shaffer, A. L. Mihalchik, W. P. Chisholm, M. E. Andrew, D. Schwegler-Berry, V. Castranova, P. Demokritou and Y. Qian, Toxicological Assessment of CoO and La2O3 Metal Oxide Nanoparticles in Human Small Airway Epithelial Cells, *Toxicol. Sci.*, 2016, **150**, 418–428.

30 J. D. Sisler, S. V. Pirela, S. Friend, M. Farcas, D. Schwegler-Berry, A. Shvedova, V. Castranova, P. Demokritou and Y. Qian, Small airway epithelial cells exposure to printer-emitted engineered nanoparticles induces cellular effects on human microvascular endothelial cells in an alveolar-capillary co-culture model, *Nanotoxicology*, 2015, **9**, 769–779.

31 I. R. Miousse, M.-C. G. Chalbot, R. Pathak, X. Lu, E. Nzabarushimana, K. Krager, N. Aykin-Burns, M. Hauer-Jensen, P. Demokritou, I. G. Kavouras and I. Koturbash, In Vitro Toxicity and Epigenotoxicity of Different Types of Ambient Particulate Matter, *Toxicol. Sci.*, 2015, **148**, 473–487.

32 J. Ma, R. R. Mercer, M. Barger, D. Schwegler-Berry, J. M. Cohen, P. Demokritou and V. Castranova, Effects of amorphous silica coating on cerium oxide nanoparticles induced pulmonary responses, *Toxicol. Appl. Pharmacol.*, 2015, **288**, 63–73.

33 X. Lu, I. R. Miousse, S. V. Pirela, J. K. Moore, S. Melnyk, I. Koturbash and P. Demokritou, In vivo epigenetic effects induced by engineered nanomaterials: A case study of copper oxide and laser printer-emitted engineered nanoparticles, *Nanotoxicology*, 2016, **10**, 629–639.

34 X. Lu, I. R. Miousse, S. V. Pirela, S. Melnyk, I. Koturbash and P. Demokritou, Short-term exposure to engineered nanomaterials affects cellular epigenome, *Nanotoxicology*, 2016, **10**, 140–150.

35 G. DeLoid, B. Casella, S. Pirela, R. Filoramo, G. Pyrgiotakis, P. Demokritou and L. Kobzik, Effects of engineered nanomaterial exposure on macrophage innate immune function, *NanoImpact*, 2016, **2**, 70–81.

36 D. J. McClements, G. DeLoid, G. Pyrgiotakis, J. A. Shatkin, H. Xiao and P. Demokritou, The role of the food matrix and gastrointestinal tract in the assessment of biological properties of ingested engineered nanomaterials (iENMs): State of the science and knowledge gaps, *NanoImpact*, 2016, **3–4**, 47–57.

37 B. A. Koeneman, Y. Zhang, P. Westerhoff, Y. Chen, J. C. Crittenden and D. G. Capco, Toxicity and cellular responses of intestinal cells exposed to titanium dioxide, *Cell Biol. Toxicol.*, 2010, **26**, 225–238.

38 Z. Guo, N. J. Martucci, F. Moreno-Olivas, E. Tako and G. J. Mahler, Titanium dioxide nanoparticle ingestion alters nutrient absorption in an in vitro model of the small intestine, *NanoImpact*, 2017, **5**, 70–82.

39 M. I. Setyawati, C. Sevencan, B.-H. Bay, J. Xie, Y. Zhang, P. Demokritou and D. T. Leong, Nano-TiO2 drives epithelial - mesenchymal transition in intestinal epithelial cancer cells, *Small*, 2018, **14**, e1800922.

40 I. S. Sohal, K. S. O'Fallon, P. Gaines, P. Demokritou and D. Bello, Ingested engineered nanomaterials: state of science in nanotoxicity testing and future research needs, *Part. Fibre Toxicol.*, 2018, **15**, 29.

41 S. Nallanthighal, C. Chan, D. J. Bharali, S. A. Mousa, E. Vásquez and R. Reliene, Particle coatings but not silver ions mediate genotoxicity of ingested silver nanoparticles in a mouse model, *NanoImpact*, 2017, **5**, 92–100.

42 H. Chen, R. Zhao, B. Wang, C. Cai, L. Zheng, H. Wang, M. Wang, H. Ouyang, X. Zhou, Z. Chai, Y. Zhao and W. Feng, The effects of orally administered Ag, TiO2 and SiO2 nanoparticles on gut microbiota composition and colitis induction in mice, *NanoImpact*, 2017, **8**, 80–88.

 This journal is © The Royal Society of Chemistry 2021

Published on 20 July 2021. Downloaded by Fail Open on 7/23/2025 9:11:29 AM.

43 X. Jiang, Y. Wu, P. Gray, J. Zheng, G. Cao, H. Zhang, X. Zhang, M. Boudreau, T. R. Croley, C. Chen and J.-J. Yin, Influence of gastrointestinal environment on free radical generation of silver nanoparticles and implications for their cytotoxicity, *NanoImpact*, 2018, **10**, 144–152.

44 B. Jovanović, N. Jovanović, V. J. Cvetković, S. Matić, S. Stanić, E. M. Whitley and T. L. Mitrović, The effects of a human food additive, titanium dioxide nanoparticles E171, on Drosophila melanogaster - a 20 generation dietary exposure experiment, *Sci. Rep.*, 2018, **8**, 17922.

45 H. Proquin, C. Rodríguez-Ibarra, C. G. J. Moonen, I. M. Urrutia Ortega, J. J. Briedé, T. M. de Kok, H. van Loveren and Y. I. Chirino, Titanium dioxide food additive (E171) induces ROS formation and genotoxicity: contribution of micro and nano-sized fractions, *Mutagenesis*, 2017, **32**, 139–149.

46 G. M. DeLoid, X. Cao, R. M. Molina, D. I. Silva, K. Bhattacharya, K. W. Ng, S. C. J. Loo, J. D. Brain and P. Demokritou, Toxicological effects of ingested nanocellulose in in vitro intestinal epithelium and in vivo rat models, *Environ. Sci.: Nano*, 2019, **6**(7), DOI: 10.1039/C9EN00184K.

47 Y. J. Lin, J. A. Shatkin and F. Kong, Evaluating mucoadhesion properties of three types of nanocellulose in the gastrointestinal tract in vitro and ex vivo, *Carbohydr. Polym.*, 2019, **210**, 157–166.

48 Z. Guo, X. Cao, G. M. Deloid, K. Sampathkumar, K. W. Ng, S. C. J. Loo and P. Demokritou, Physicochemical and Morphological Transformations of Chitosan Nanoparticles across the Gastrointestinal Tract and Cellular Toxicity in an in Vitro Model of the Small Intestinal Epithelium, *J. Agric. Food Chem.*, 2020, **68**(1), DOI: 10.1021/acs.jafc.9b05506.

49 G. M. DeLoid, Y. Wang, K. Kapronezai, L. R. Lorente, R. Zhang, G. Pyrgiotakis, N. V. Konduru, M. Ericsson, J. C. White, R. De La Torre-Roche, H. Xiao, D. J. McClements and P. Demokritou, An integrated methodology for assessing the impact of food matrix and gastrointestinal effects on the biokinetics and cellular toxicity of ingested engineered nanomaterials, *Part. Fibre Toxicol.*, 2017, **14**, 40.

50 Z. Zhang, R. Zhang, H. Xiao, K. Bhattacharya, D. Bitounis, P. Demokritou and D. J. McClements, Development of a standardized food model for studying the impact of food matrix effects on the gastrointestinal fate and toxicity of ingested nanomaterials, *NanoImpact*, 2019, **13**, 13–25.

51 K. Bhattacharya, G. Kiliç, P. M. Costa and B. Fadeel, Cytotoxicity screening and cytokine profiling of nineteen nanomaterials enables hazard ranking and grouping based on inflammogenic potential, *Nanotoxicology*, 2017, **11**, 809–826.

52 A. L. Menas, N. Yanamala, M. T. Farcas, M. Russo, S. Friend, P. M. Fournier, A. Star, I. Iavicoli, G. V. Shurin, U. B. Vogel, B. Fadeel, D. Beezhold, E. R. Kisin and A. A. Shvedova, Fibrillar vs crystalline nanocellulose pulmonary epithelial cell responses: Cytotoxicity or inflammation?, *Chemosphere*, 2017, **171**, 671–680.

53 C. Endes, S. Camarero-Espinosa, S. Mueller, E. J. Foster, A. Petri-Fink, B. Rothen-Rutishauser, C. Weder and M. J. D. Clift, A critical review of the current knowledge regarding the biological impact of nanocellulose, *J. Nanobiotechnol.*, 2016, **14**, 78.

54 S. Khare, G. M. DeLoid, R. M. Molina, K. Gokulan, S. P. Couvillion, K. J. Bloodsworth, E. K. Eder, A. R. Wong, D. W. Hoyt, L. M. Bramer, T. O. Metz, B. D. Thrall, J. D. Brain and P. Demokritou, Effects of ingested nanocellulose on intestinal microbiota and homeostasis in Wistar Han rats, *NanoImpact*, 2020, **18**, DOI: 10.1016/j.impact.2020.100216.

55 L. Liu and F. Kong, Influence of nanocellulose on in vitro digestion of whey protein isolate, *Carbohydr. Polym.*, 2019, **210**, 399–411.

56 L. Liu and F. Kong, The behavior of nanocellulose in gastrointestinal tract and its influence on food digestion, *J. Food Eng.*, 2021, **292**, 110346.

57 J. Nsor-Atindana, H. Douglas Goff, W. Liu, M. Chen and F. Zhong, The resilience of nanocrystalline cellulose viscosity to simulated digestive processes and its influence on glucose diffusion, *Carbohydr. Polym.*, 2018, **200**, 436–445.

58 N. Ji, C. Liu, M. Li, Q. Sun and L. Xiong, Interaction of cellulose nanocrystals and amylase: Its influence on enzyme activity and resistant starch content, *Food Chem.*, 2018, **245**, 481–487.

59 L. Liu, W. L. Kerr, F. Kong, D. R. Dee and M. Lin, Influence of nano-fibrillated cellulose (NFC) on starch digestion and glucose absorption, *Carbohydr. Polym.*, 2018, **196**, 146–153.

60 D. R. M. Andrade, M. H. Mendonça, C. V. Helm, W. L. E. Magalhães, G. I. B. de Muniz and S. G. Kestur, Assessment of Nano Cellulose from Peach Palm Residue as Potential Food Additive: Part II: Preliminary Studies, *J. Food Sci. Technol.*, 2015, **52**, 5641–5650.

61 Y. Chen, Y. J. Lin, T. Nagy, F. Kong and T. L. Guo, Subchronic exposure to cellulose nanofibrils induces nutritional risk by non-specifically reducing the intestinal absorption, *Carbohydr. Polym.*, 2020, **229**, DOI: 10.1016/j.carbpol.2019.115536.

62 G. Pyrgiotakis, W. Luu, Z. Zhang, N. Vaze, G. DeLoid, L. Rubio, W. A. C. Graham, D. C. Bell, D. Bousfield and P. Demokritou, Development of high throughput, high precision synthesis platforms and characterization methodologies for toxicological studies of nanocellulose, *Cellulose*, 2018, **25**, 2303–2319.

63 K. Sampathkumar and S. C. J. Loo, Targeted Gastrointestinal Delivery of Nutraceuticals with Polysaccharide-Based Coatings, *Macromol. Biosci.*, 2018, **18**, 1700363.

64 World Health Organization, *The international pharmacopoeia*, 2012.

65 J. Beltran-Huarac, Z. Zhang, G. Pyrgiotakis, G. DeLoid, N. Vaze and P. Demokritou, Development of reference metal and metal oxide engineered nanomaterials for nanotoxicology research using high throughput and precision flame spray synthesis approaches, *NanoImpact*, 2018, **10**, 26–37.

Published on 20 July 2021. Downloaded by Fail Open on 7/23/2025 9:11:29 AM.

66 J. Cohen, G. Deloid, G. Pyrgiotakis and P. Demokritou, Interactions of engineered nanomaterials in physiological media and implications for in vitro dosimetry, *Nanotoxicology*, 2013, **7**, 417–431.

67 J. M. Cohen, J. Beltran-Huarac, G. Pyrgiotakis and P. Demokritou, Effective delivery of sonication energy to fast settling and agglomerating nanomaterial suspensions for cellular studies: Implications for stability, particle kinetics, dosimetry and toxicity, *NanoImpact*, 2018, **10**, 81–86.

68 Z. Guo, N. J. Martucci, Y. Liu, E. Yoo, E. Tako and G. J. Mahler, Silicon dioxide nanoparticle exposure affects small intestine function in an in vitro model, *Nanotoxicology*, 2018, **12**, 485–508.

69 J. C. Pickup, F. Hussain, N. D. Evans, O. J. Rolinski and D. J. S. Birch, Fluorescence-based glucose sensors, *Biosens. Bioelectron.*, 2005, **20**, 2555–2565.

70 J. Tao, R. K. Diaz, R. V. Teixeira and T. J. Hackmann, Transport of a Fluorescent Analogue of Glucose (2-NBDG) versus Radiolabeled Sugars by Rumen Bacteria and Escherichia coli, *Biochemistry*, 2016, **55**(18), 2578–2587.

71 S. Page, A. Munsell and A. J. Al Ahmad, Cerebral hypoxia/ischemia selectively disrupts tight junctions complexes in stem cell - derived human brain microvascular endothelial cells, *Fluids Barriers CNS*, 2016, 1–10.

72 M. Ryou, G. Roy, A. Winters, L. Xie, R. T. Mallet and S. Yang, Pyruvate minimizes rtPA toxicity from in vitro oxygen-glucose deprivation and reoxygenation, *Brain Res.*, 2013, **1530**, 66–75.

73 M. Prentki, C. Guay, S. R. M. Madiraju and A. Aumais, A Role for ATP-Citrate Lyase, Malic Enzyme, and Pyruvate/Citrate Cycling in Glucose-induced Insulin Secretion *, *J. Biol. Chem.*, 2007, **282**(49), 35657–35665.

74 D. Bitounis, G. Pyrgiotakis, D. Bousfield and P. Demokritou, Dispersion preparation, characterization, and dosimetric analysis of cellulose nano-fibrils and nano-crystals: Implications for cellular toxicological studies, *NanoImpact*, 2019, **15**, DOI: 10.1016/j.impact.2019.100171.

75 E. M. Wright, D. D. F. L. LOO and B. A. Hirayama, Biology of human sodium glucose transporters, *Physiol. Rev.*, 2011, **91**, 733–794.

76 A. Leturque, E. Brot-Laroche, M. Le Gall, E. Stolarczyk and V. Tobin, The role of GLUT2 in dietary sugar handling, *J. Physiol. Biochem.*, 2005, **61**(4), 529–537.

77 L. Chen, B. Tuo and H. Dong, Regulation of intestinal glucose absorption by ion channels and transporters, *Nutrients*, 2016, **8**(1).

78 P. V. Röder, K. E. Geillinger, T. S. Zietek, B. Thorens, H. Koepsell and H. Daniel, The role of SGLT1 and GLUT2 in intestinal glucose transport and sensing, *PLoS One*, 2014, **9**(2), DOI: 10.1371/journal.pone.0089977.

79 C. Pires, J. A. P. Vilela and C. Airoldi, The Effect of Chitin Alkaline Deacetylation at Different Condition on Particle Properties, *Procedia Chem.*, 2014, **9**, 220–225.

80 S. M. Ahsan, M. Thomas, K. K. Reddy, S. G. Sooraparaju, A. Asthana and I. Bhatnagar, Chitosan as biomaterial in drug delivery and tissue engineering, *Int. J. Biol. Macromol.*, 2018, **110**, 97–109.

 This journal is © The Royal Society of Chemistry 2021